Supporting information

The Structural Basis of the Inhibition of Golgi α–Mannosidase II by Mannostatin A and the Role of the Thiomethyl Moiety in Ligand-Protein Interactions

Sameer P. Kawatkar, Douglas A Kuntz, Robert J. Woods, David R. Rose* and Geert-Jan Boons*

Table 1S: Statistics for Data Collection and Refinement

Complex with:	**Manostatin A**	**Benzyl-Mannostatin**
PDB code	**2F7O**	**2F7P**
HET symbol	MSN	SK2
Space Group		
Cell dimensions (Å)	69.00/109.30/138.35	68.95/109.87/139.04
Data Collection (values in parenthesis represent high resolution shell)		
Resolution (Å)	30-1.45 (1.48-1.45)	30-1.28 (1.31-1.28)
Unique Reflections/Redundancy	181,459/4.1	266,693/6.7
I/sigma I	12.3 (2.9)	16.6 (2.7)
% Completeness	97.1 (92.3)	97.7 (79.8)
R merge	0.10 (0.463)	0.10 (0.575)
Wilson B ($Å^2$)	14.5	11.1
Structure Refinement		
R_{workt}/R_{free} (reflections for R_{free})	0.206/0.235 (4103)	0.166/0.180 (4884)
Amino Acids/Alternate conformers	1014/11	1014/37
Water Molecules	1048	1226
rmsd bonds (Å)	0.0203	0.017
rmsd angles (°)	2.0	1.8
AverageBFactor ($Å^2$)		
Overall	16.9	13.8
Protein Main Chain	14.6	10.7
Protein Side Chain	16.7	13.6
Water	26.6	24.9
Inhibitor	8.7	12.0
Zn	8.4	5.9
MPD	21.5	13.6
PO_4	30.5	-

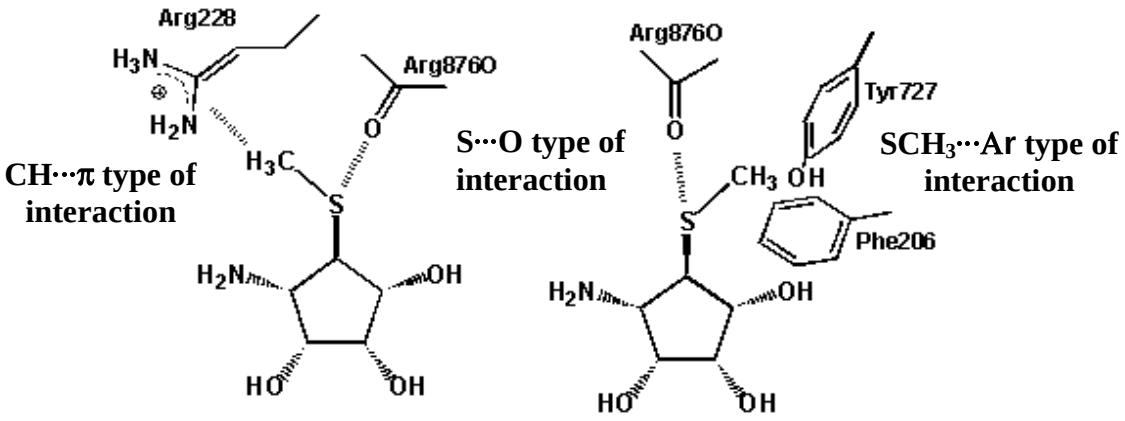

Figure 1S. Different thiomethyl interactions in cf1 and cf2 conformation of methyl carbon atom, as observed in the X-ray structures of Mannostatin A complexed with dGMII.

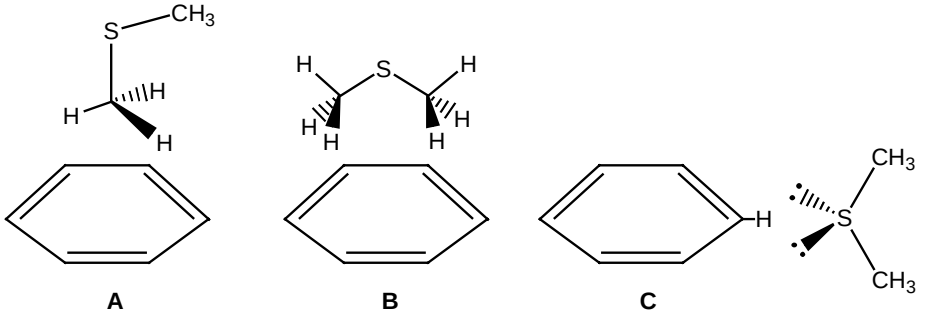

Figure 2S. Different models studied using ab initio calculations by Pranata. These models gave the estimates of the contribution of thiomethyl interaction with the benzene ring towards the stability of the system.

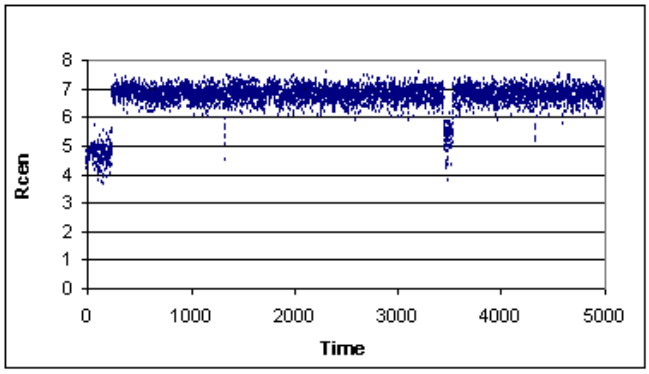

Figure 3S. Plot of distance between the centroid of the phenyl ring in 2 and the sulfur atom in 2 as a function of time, in 5-ns trajectory for MD simulation of free ligand in water. The plot indicates that the intramolecular interaction observed in the X-ray structure may not be strong interaction.

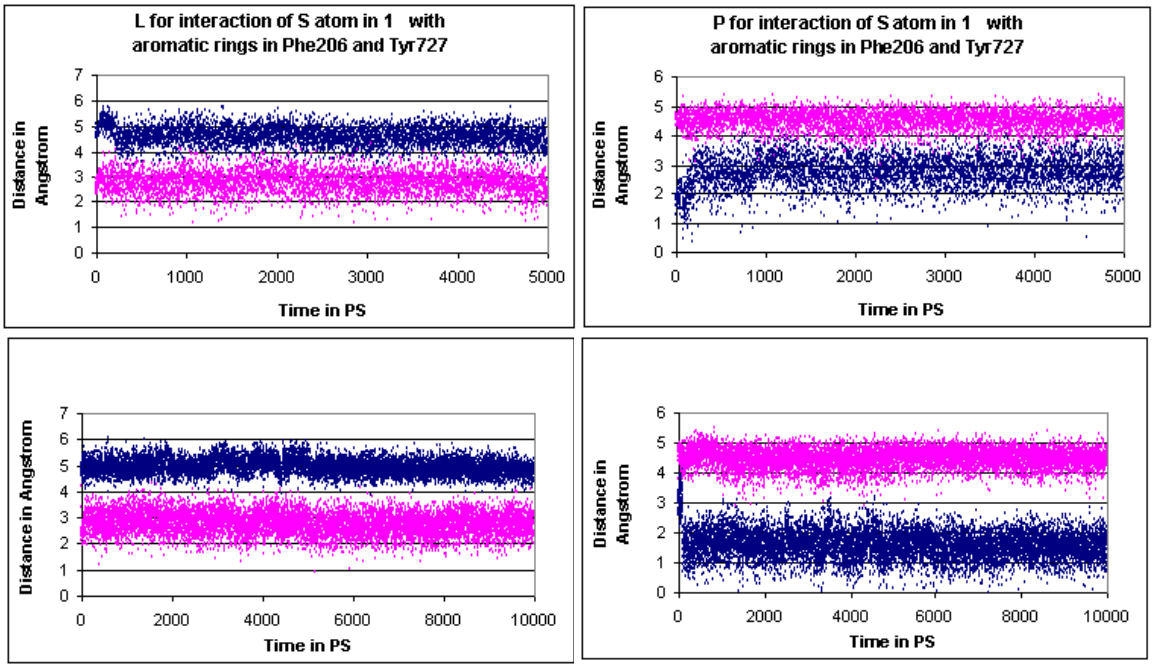

Figure 4S. Plots of perpendicular (P) and horizontal distance (L) between the sulfur atoms in **1** and **2**, and the centroid of the phenyl ring in Phe206 and Tyr727 (blue – Phe206 and magenta – Tyr727) as a function of time in 10-ns trajectories of ligand-protein complexes. These plots indicate that the interactions made by thiomethyl ether with the Phe206 and Tyr727 are retained.

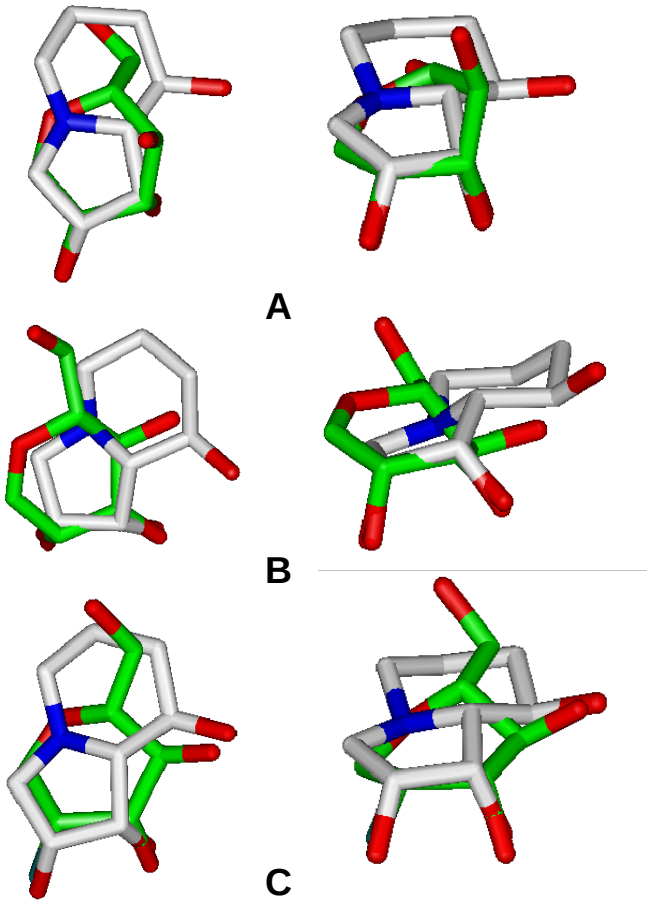

Figure 5S. Overlays of swainsonine (in bound conformation) with flap-up (A) and flap-down (B) oxacarbenium, and covalent intermediate (C, PDB ID 1QX1).

Complete references.

55. Case, D. A.; Pearlman, D. A.; Caldwell, J. W.; Cheatham III, T. E.; Wang, J.; Ross, W. S.; Simmerling, C. L.; Merz, K. M.; Stanton, R. V.; Cheng, A. L.; Vincent, J. J.; Crowley, M.; Tsui, V.; Radmer, R. J.; Duan, Y.; Pitera, J.; Massova, I.; Seibel, G. L.; Singh, P. K. W.; Kollman, P. A. *Amber 7.0*, University of California: San Francisco, CA, 2002.

59. Frisch, M. J.; Trucks, G. W.; Schlegel, H. B.; Scuseria, G. E.; Robb, M. A.; Cheeseman, J. R.; Zakrzewski, V. G.; Montgomery, J. A.; Stratmann, J., R. E.; Burant, J. C.; Dapprich, S.; Millam, J. M.; Daniels, A. D.; Kudin, K. N.; Strain, M. C.; Farkas, O.; Tomasi, J.; Barone, V.; Cossi, M.; Cammi, R.; Mennucci, B.; Pomelli, C.; Adamo, C.; Clifford, S.; Ochterski, J.; Petersson, G. A.; Ayala, P. Y.; Cui, Q.; Morokuma, K.; Malick, D. K.; Rabuck, A. D.; Raghavachari, K.; Foresman, J. B.; Cioslowski, J.; Ortiz, J. V.; Baboul, A. G.; Stefanov, B. B.; Liu, G.; Liashenko, A.; Piskorz, P.; Komaromi, I.; Gomperts, R.; Martin, R. L.; Fox, D. J.; Keith, T.; Al-Laham, M. A.; Peng, C. Y.; Nanayakkara, A.; Challacombe, M.; Gill, P. M. W.; Johnson, B.; Chen, W.; Wong, M. W.; Andres, J. L.; Gonzalez, C.; Head-Gordon, M.; Replogle, E. S.; Pople, J. A. *Gaussian 98*, Revision A.11.3 ed; Gaussian, Inc.: Pittsburgh, PA, 2002.